A 2D FINITE ELEMENT/1D FOURIER SOLUTION TO THE FOKKER-PLANCK EQUATION

Andy Spencer

Utah State University

NIMROD meeting
June 14, 2012

Outline

- Analytics - Physics of the Fokker-Planck Equation
- Numerics - Solving the Fokker-Planck Equation
- Applications
    - Test Particle Calculations
    - Test and Field Particle Calculations

The Fokker-Planck Equation

Evolution of f_a governed by

$$\frac{\partial f_a}{\partial t} + \mathbf{v}\cdot\nabla f_a + \frac{q_a}{m_a}\left(\mathbf{E}+\mathbf{v}\times\mathbf{B}\right)\cdot\nabla_{\mathbf{v}} f_a = \sum_b C\left(f_a, f_b\right)$$

$$= -\nabla_{\mathbf{v}}\cdot\sum_b \frac{\Gamma_{ab}}{2}\left[\frac{m_a+m_b}{m_b}\left(\nabla_{\mathbf{v}}\cdot\mathsf{D}_b\right)f_a - \nabla_{\mathbf{v}}\cdot\left(\mathsf{D}_b f_a\right)\right]$$

where

$$\Gamma_{ab} = \frac{q_a^2 q_b^2 \ln\Lambda_{ab}}{4\pi\varepsilon_0^2 m_a^2}, \qquad \ln\Lambda_{ab} = \ln\left(\frac{r_{\max}}{r_{\min}}\right)$$

and

$$\mathsf{D}_b\left(\mathbf{v},t\right) = \int d\mathbf{v}' f_b\left(\mathbf{v}',t\right)\mathsf{U}, \qquad \mathsf{U} = \frac{u^2\mathsf{I}-\mathbf{uu}}{u^3}$$

δf-linearization about a Maxwellian

Linearize about a *static* Maxwellian distribution

$$f_a(\mathbf{v},t) = f_a^{\mathrm{M}}(\mathbf{v}) + F_a(\mathbf{v},t)$$

$$\frac{\partial F_a}{\partial t} = \sum_b C\left(F_a, f_b^{\mathrm{M}}\right)$$

δf-linearization about a Maxwellian

Linearize about a *static* Maxwellian distribution

$$f_a(\mathbf{v},t) = f_a^{\mathrm{M}}(\mathbf{v}) + F_a(\mathbf{v},t)$$

$$\frac{\partial F_a}{\partial t} = \sum_b C\left(F_a, f_b^{\mathrm{M}}\right)$$

$$\downarrow$$

$$\frac{\partial F_a}{\partial t} = \nabla_{\mathbf{v}} \cdot \sum_b \frac{\Gamma_{ab}}{2} \left[\left(\frac{2}{v_{Tb}} \frac{m_a}{m_b} \mathbf{z}_b F_a + \nabla_{\mathbf{v}} F_a \right) \cdot \mathsf{D}_b^{\mathrm{M}} \right]$$

δf-linearization about a Maxwellian

Test particle operator

$$\frac{\partial F_a}{\partial t} = \nabla_{\mathbf{v}} \cdot \sum_b \frac{\Gamma_{ab}}{2} \left[\left(\frac{2}{v_{Tb}} \frac{m_a}{m_b} \mathbf{z}_b F_a + \nabla_{\mathbf{v}} F_a \right) \cdot \mathsf{D}_b^{\mathrm{M}} \right]$$

where

$$\mathsf{D}_b^{\mathrm{M}} = \frac{n_b}{v_{Tb}} \left[\frac{3G(z_b) - E(z_b)}{z_b^3} \mathbf{z}_b \mathbf{z}_b + \frac{E(z_b) - G(z_b)}{z_b} \mathsf{I} \right],$$

$\mathbf{z}_b = \frac{\mathbf{v} - \mathbf{V}_b}{v_{Tb}}$, $G(z_b) = \frac{E(z_b)}{2z_b^2} - \frac{e^{-z_b^2}}{\sqrt{\pi} z_b}$ is the Chandrasekhar function, and $E(z_b) = \frac{2}{\sqrt{\pi}} \int_0^{z_b} dx e^{-x^2}$ is the error function.

The Chapman-Enskog-like Approach

Now let the Maxwellian be time dependent

$$\begin{aligned} f_a(\mathbf{v},t) &= f_a^{\mathrm{M}}(\mathbf{v},t) + F_a(\mathbf{v},t) \\ \frac{\partial f_a}{\partial t} &= \sum_b \left[C\left(f_a^{\mathrm{M}}, f_b^{\mathrm{M}}\right) + C\left(F_a, f_b^{\mathrm{M}}\right) + C\left(f_a^{\mathrm{M}}, F_b\right) \right] \end{aligned}$$

By using the fluid equations we can replace:

$$\frac{\partial f_a^{\mathrm{M}}}{\partial t} = \frac{2 f_a^{\mathrm{M}}}{n_a m_a v_{Ta}} \sum_b \left[\mathbf{z}_a \cdot \mathbf{R}_{ab} + \frac{Q_{ab}}{v_{Ta}} \left(\frac{2}{3} z_a^2 - 1 \right) \right]$$

Conservation Laws of Coulomb Collision Operator

$$\begin{aligned}\mathbf{R}_{ab} &= \int d\mathbf{v} m_a \mathbf{v} C(f_a, f_b) \\ Q_{ab} &= \int d\mathbf{v} \frac{1}{2} m_a (\mathbf{v} - \mathbf{V}_a)^2 C(f_a, f_b)\end{aligned}$$

Conservation of density, momentum and energy

$$\begin{aligned}\int d\mathbf{v} C(f_a, f_b) &= 0 \\ \mathbf{R}_{ab} + \mathbf{R}_{ba} &= 0 \\ Q_{ab} + Q_{ba} &= \mathbf{R}_{ab} \cdot (\mathbf{V}_b - \mathbf{V}_a)\end{aligned}$$

The Field Operator

$$C\left(f_a^{\mathrm{M}}, F_b\right) = -\Gamma_{ab}\nabla_{\mathbf{v}} \cdot \left[f_a^{\mathrm{M}}\left(\frac{m_a}{m_b}\nabla_{\mathbf{v}} h_b + \frac{\mathbf{z}_a}{v_{Ta}} \cdot \nabla_{\mathbf{v}}\nabla_{\mathbf{v}} g_b\right)\right]$$

$$\begin{aligned}
h_b &= \int d\mathbf{v}' F_b\left(\mathbf{v}', t\right) u^{-1} \\
g_b &= \int d\mathbf{v}' F_b\left(\mathbf{v}', t\right) u \\
\nabla_{\mathbf{v}} h_b &= -\int d\mathbf{v}' F_b\left(\mathbf{v}', t\right) u^{-3}\mathbf{u} \\
\nabla_{\mathbf{v}}\nabla_{\mathbf{v}} g_b &= \int d\mathbf{v}' F_b\left(\mathbf{v}', t\right) \frac{u^2\mathsf{I} - \mathbf{u}\mathbf{u}}{u^3}
\end{aligned}$$

Cyclotron Motion & Cylindrical Velocity Coordinates

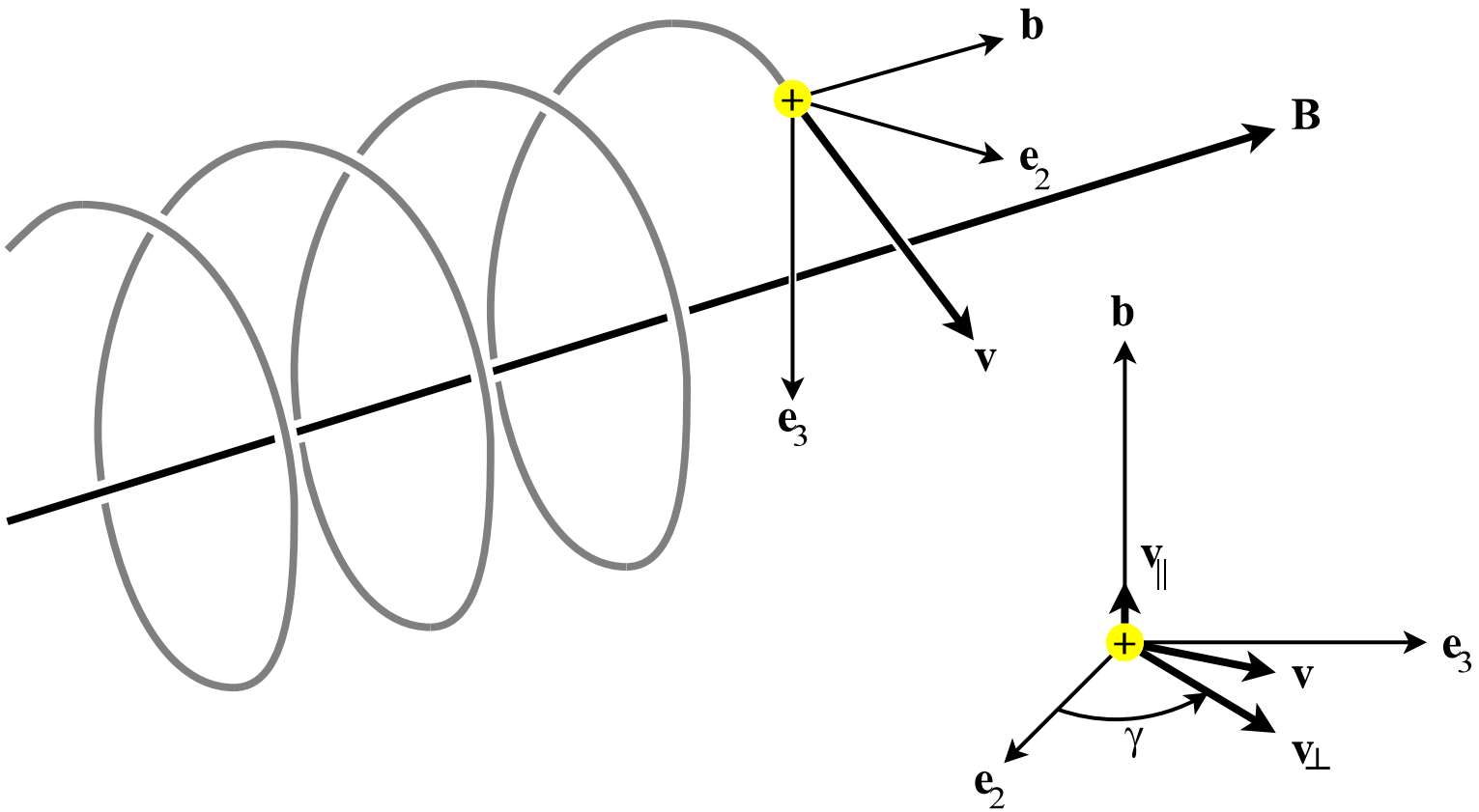

A 2D Finite Element/1D Fourier Representation

$$\mathbf{v} \rightarrow \left(v_{\parallel}, v_{\perp}, \gamma\right),$$

$$\mathbf{c}_a \equiv \mathbf{v} / v_{Ta},$$

$$F_a = \sum_{n=-N}^{N} \sum_{j=1}^{J} F_{a,j,n}\left(t\right) \alpha_j \left(c_{a\parallel}, c_{a\perp}\right) \mathrm{e}^{in\gamma}$$

Finite Element Grid in Velocity Space

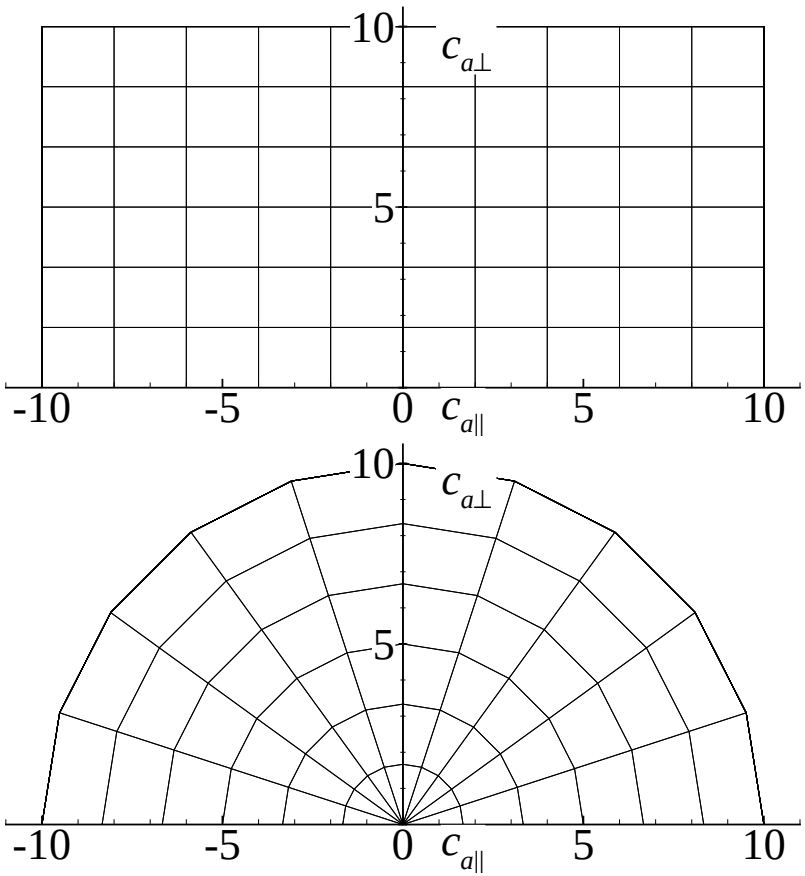

Figure: Example 6×10 grids.

The coordinates themselves are expanded in the finite element basis:

$$c_{a\parallel} = \sum_{i=1}^{I} c_{a\parallel,i}\alpha_i(x,y),$$

$$c_{a\perp} = \sum_{i=1}^{I} c_{a\perp,i}\alpha_i(x,y).$$

θ-centered Implicit Time Advance

For a linear integro-differential operator, $\mathbb{O}$,

$$\frac{\partial F}{\partial t} = \mathbb{O}\left(F\right) \longrightarrow \frac{\Delta F}{\Delta t} = \mathbb{O}\left(F^{k+\theta}\right),$$

where

$$\begin{aligned} \Delta F &= F^{k+1} - F^{k}, \\ \Delta t &= t^{k+1} - t^{k}, \\ F^{k+\theta} &= F^{k} + \theta \Delta F, \end{aligned}$$

and

$$\theta = 0, 0.5, 1.$$

Weak Formulation

Procedure to obtain system of equations

Take inner product of FP equation and test functions, $\alpha_j e^{-in'\gamma}$, then integrate by parts to ensure C^0 continuity.

$$
\begin{array}{ccc}
\Delta F - \theta \Delta t \, \mathbb{O}\left(\Delta F\right) & = & \Delta t \, \mathbb{O}\left(F^k\left(\mathbf{v}\right)\right) \\
\downarrow & & \downarrow \\
\int d\mathbf{c}_a \frac{1}{2\pi} \alpha_j e^{-in'\gamma} \times & & \int d\mathbf{c}_a \frac{1}{2\pi} \alpha_j e^{-in'\gamma} \times \\
\downarrow & & \downarrow \\
\text{Partial integration} & & \text{Partial integration} \\
\downarrow & & \downarrow \\
\mathbf{A} \cdot \Delta \mathbf{F} & = & \mathbf{b}
\end{array}
$$

Weak Formulation of the Test Particle Operator

Right side of matrix equation:

$$-\frac{\Delta t}{2\pi v_{Ta}}\sum_b \frac{\Gamma_{ab}}{2}\int_\Omega d\mathbf{c}_a \mathrm{e}^{-in'\gamma}\overrightarrow{\alpha_j^{n'}}\cdot\left[\left(\frac{2}{v_{Tb}}\frac{m_a}{m_b}\mathbf{z}_b F_a^k+\frac{1}{v_{Ta}}\nabla_{\mathbf{c}_a}F_a^k\right)\cdot \mathsf{D}_b^{\mathrm{M}}\right]$$

Left side of matrix equation:

$$\int_\Omega dc_{a\parallel}dc_{a\perp}c_{a\perp}\alpha_j\Delta F_{a,n'}$$
$$+\frac{\theta\Delta t}{2\pi v_{Ta}}\sum_b \frac{\Gamma_{ab}}{2}\int_\Omega d\mathbf{c}_a \mathrm{e}^{-in'\gamma}\overrightarrow{\alpha_j^{n'}}\cdot\left[\left(\frac{2}{v_{Tb}}\frac{m_a}{m_b}\mathbf{z}_b \Delta F_a+\frac{1}{v_{Ta}}\nabla_{\mathbf{c}_a}\Delta F_a\right)\cdot \mathsf{D}_b^{\mathrm{M}}\right]$$

where

$$\overrightarrow{\alpha_j^{n'}}\equiv \mathrm{e}^{in'\gamma}\nabla_{\mathbf{c}_a}\left(\alpha_j \mathrm{e}^{-in'\gamma}\right)$$

Initial Conditions

- Initial ion test particle distribution is Maxwellian
- $n_\mathrm{i} = 10^{20}\,\mathrm{m}^{-3}$, $n_\mathrm{test} = 10^{18}\,\mathrm{m}^{-3}$ and $T_\mathrm{test} \equiv 1.5\,\mathrm{keV}$
- $T_\mathrm{i} = 2.250\,\mathrm{keV}$ for heating, or $1.125\,\mathrm{keV}$ for cooling
- Assuming F_i remains Maxwellian during the thermalization process, the temperature evolves as

$$\frac{dT_\mathrm{test}}{dt} = -\frac{8}{3\sqrt{\pi}} \frac{T_\mathrm{test} - T_\mathrm{i}}{\tau_l^{\mathrm{i/i}}} \tag{1}$$

where $\tau_l^{\mathrm{i/i}}(\varepsilon) = \frac{\sqrt{m_\mathrm{i}}}{\pi\sqrt{2}q_\mathrm{i}^4} \frac{\varepsilon^{3/2}}{\ln\Lambda_c n_\mathrm{i}}$, and $\varepsilon = T_\mathrm{test} + T_\mathrm{i}$.

Numerical Results

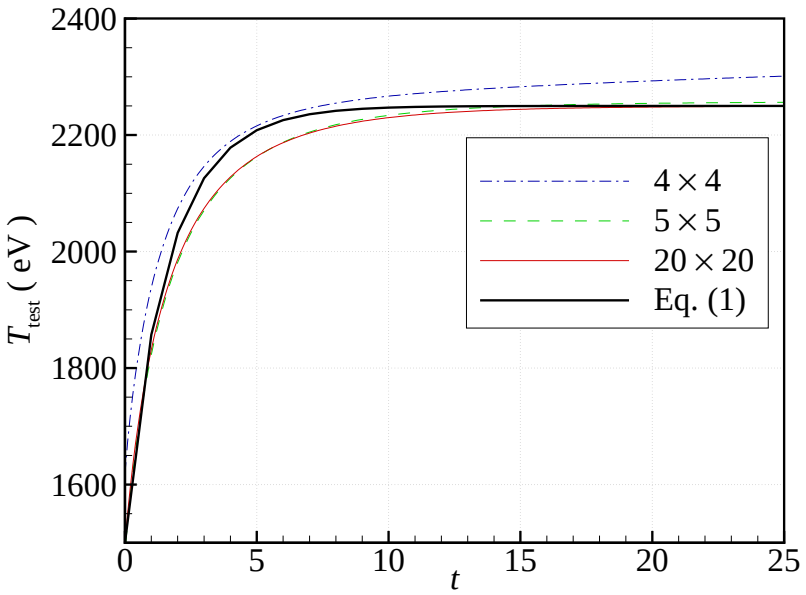

Figure: Heating of tenuous ion distribution in a 2.250 keV ion background. $p = 4$ in each case.

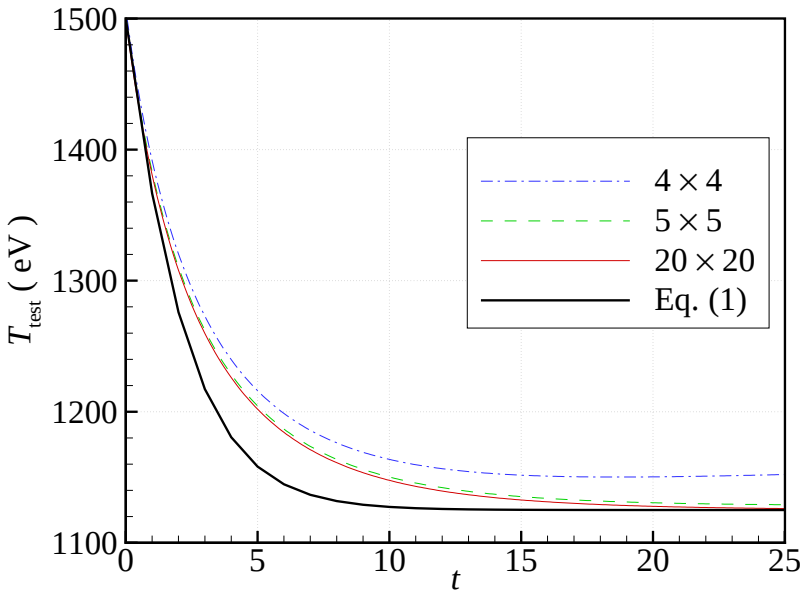

Figure: Cooling of tenuous ion distribution in a 1.125 keV ion background. $p = 4$ in each case.

Comparison of Degrees of Freedom

Xiong et al. did thermalization problem using

- Finite-volume with coordinates (μ, E)
- $E_{\max} = \mu_{\max} = 16$ and external magnetic field, $B = 1.2\,\mathrm{T}$
- Roughly corresponds to $\left(c_{\mathrm{i}\perp\max}, c_{\mathrm{i}\parallel\max}\right) = (5,5)$
- 4^{th} order polynomials (15 coefficients) in each cell

How do we compare?

- Our solution on 5×5 grid comparable to theirs on 60×60 grid
- That is 441 degrees of freedom compared to 54,000

Heating Problem Under h-type & p-type refinement

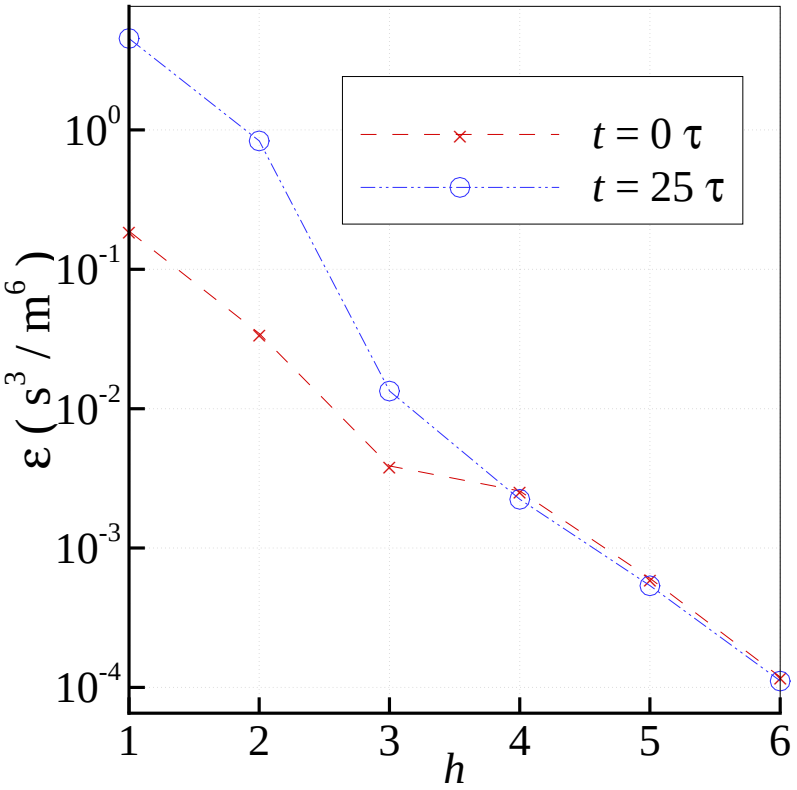

Figure: $\varepsilon(0)$ and $\varepsilon(25\,\tau)$ using a $2^h \times 2^{h+1}$ grid, $p = 1$.

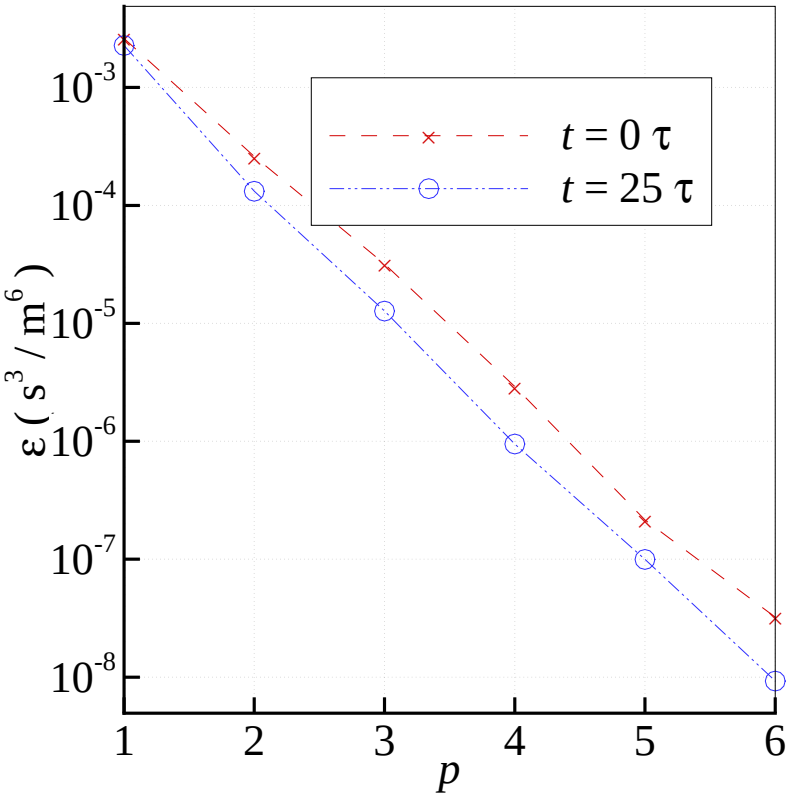

Figure: $\varepsilon(0)$ and $\varepsilon(25\,\tau)$ using a 16×32 grid under p-type refinement.

Comparing Time Advances in Heating Problem

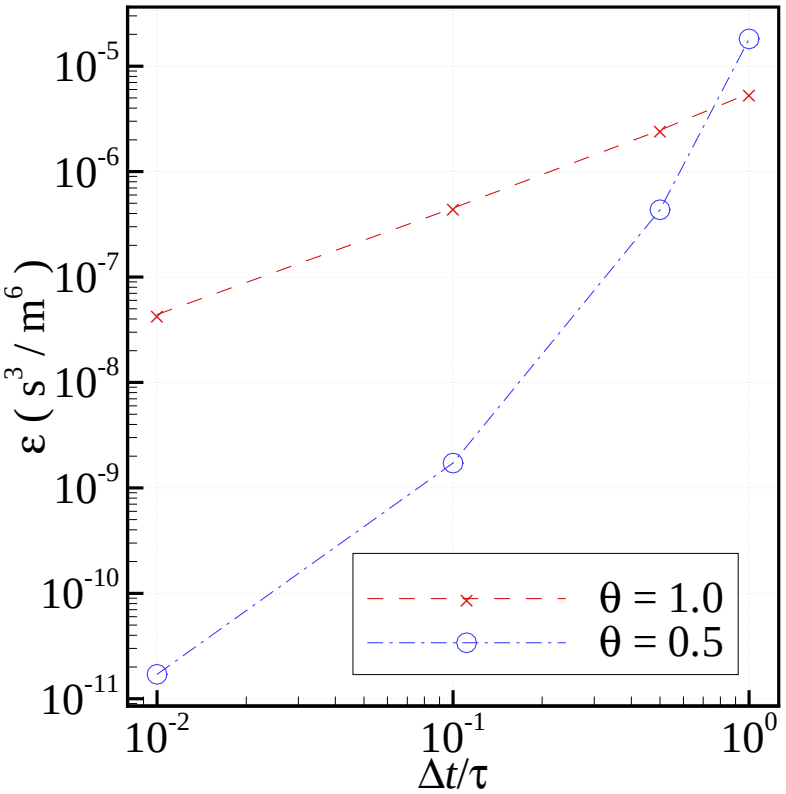

Figure: $\varepsilon\,(25\,\tau)$, with different Δt, using a 5×5 grid, and $p = 4$.

Density Conservation in Heating Problem

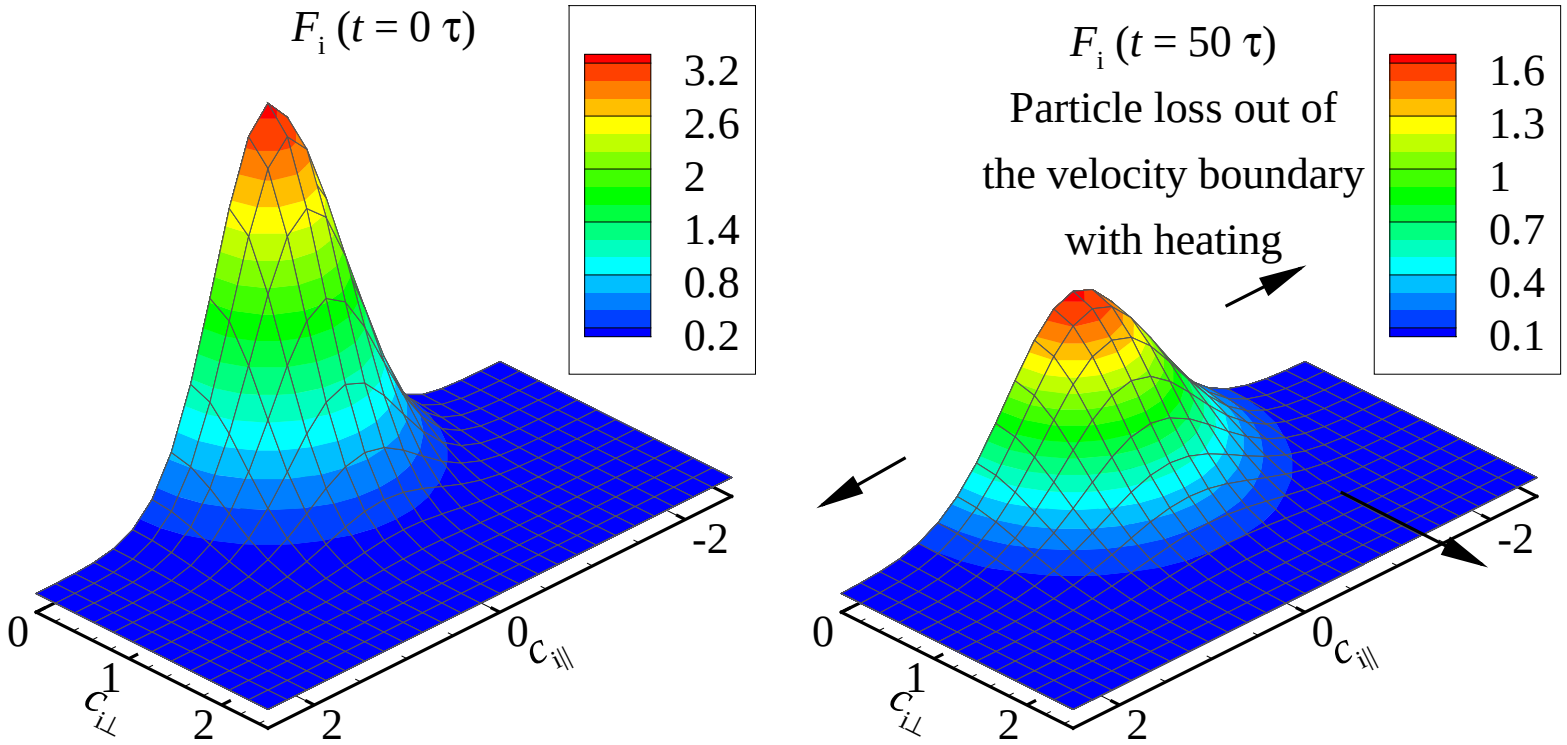

Figure: With a 4×8 grid and $p = 3$ $F_i\,(0)$ is resolved, but as particles gain energy from collisions with the warmer background some "escape" and the density decreases.

Density Conservation in Heating Problem

p	h	$c_{\mathrm{i}\perp\max}$	$\lvert c_{\mathrm{i}\parallel\max}\rvert$	$\frac{n_{\mathrm{test}}(t=50\,\tau)-n_{\mathrm{test}}(t=0\,\tau)}{n_{\mathrm{test}}(t=0\,\tau)}$
3	2	2.5	2.5	-9.82×10^{-2}
3	3	5.0	5.0	-2.11×10^{-9}
3	4	10.0	10.0	5.00×10^{-16}

Table: Increasing the velocity domain shows improved conservation in n_{test} and mitigated domain truncation error. This error for the larger domains is much smaller than the error due to the FEM representation itself $\approx 6\times10^{-6}$.

Testing the Fourier Expansion

Consider the initial conditions

$$f_{\mathrm{i}}^{\mathrm{M}}(t=0) = \frac{n_{\mathrm{i}}}{\pi^{3/2} v_{T\mathrm{i}}^3} \exp\left[-\left(\frac{\mathbf{v}-\mathbf{V}_{\mathrm{i}}}{v_{T\mathrm{i}}}\right)^2\right],$$

$$F_{\mathrm{i}}(t=0) = \frac{n_{\mathrm{test}}}{\pi^{3/2} v_{T\mathrm{i}}^3} \exp\left[-\left(\frac{\mathbf{v}}{v_{T\mathrm{i}}}\right)^2\right],$$

where $v_{T\mathrm{i}} = 3.096 \times 10^5\,\mathrm{m/s}$ ($T_{\mathrm{i}} = 1\,\mathrm{keV}$), $n_{\mathrm{i}} = 10^{20}\,\mathrm{m}^{-3}$, and $n_{\mathrm{test}} = 10^{18}\,\mathrm{m}^{-3}$.

Testing the Fourier Expansion

Recall the test particle operator

$$\frac{\partial F_a}{\partial t} = \sum_b \frac{\Gamma_{ab}}{2} \nabla_{\mathbf{v}} \cdot \left[\left(\frac{2}{v_{Tb}} \frac{m_a}{m_b} \mathbf{z}_b F_a + \nabla_{\mathbf{v}} F_a \right) \cdot \mathsf{D}_b^{\mathrm{M}} \right].$$

where

$$\mathsf{D}_b^{\mathrm{M}} = \frac{n_b}{v_{Tb}} \left[\frac{3G(z_b) - E(z_b)}{z_b^3} \mathbf{z}_b \mathbf{z}_b + \frac{E(z_b) - G(z_b)}{z_b} \mathsf{I} \right], \quad (2)$$

Testing the Fourier Expansion

- This problem requires $n > 0$ Fourier terms.
- We consider two cases: $\mathbf{V}_\mathrm{i} = 0.1\, v_{T\mathrm{i}} \hat{\mathbf{e}}_2$, and $\mathbf{V}_\mathrm{i} = v_{T\mathrm{i}} \hat{\mathbf{e}}_2$.
- We use a 16×32 mesh, $c_{\mathrm{i}\perp\mathrm{max}} = c_{\mathrm{i}\parallel\mathrm{max}} = 10$ and $p = 3$.

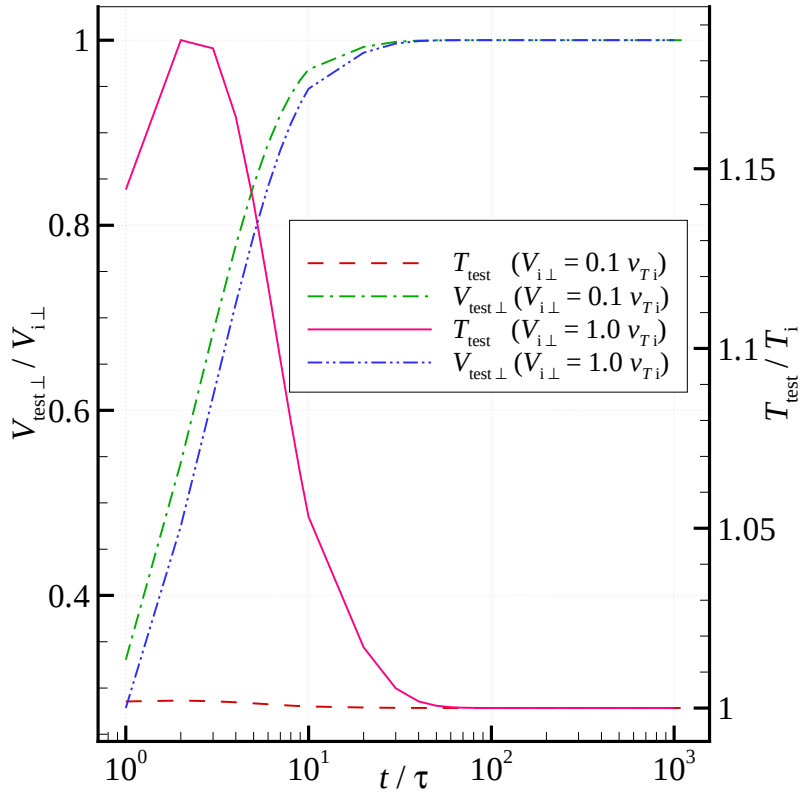

Figure: Ion flow and temperature evolution.

Testing the Fourier Expansion

- Define $\Xi_n(t) \equiv \sum_j \left| F^k_{\mathrm{i},n,j}(t) \right|$, where $j \in$ vertex nodes.
- This figure shows more Fourier modes are needed when background perpendicular flow is larger.

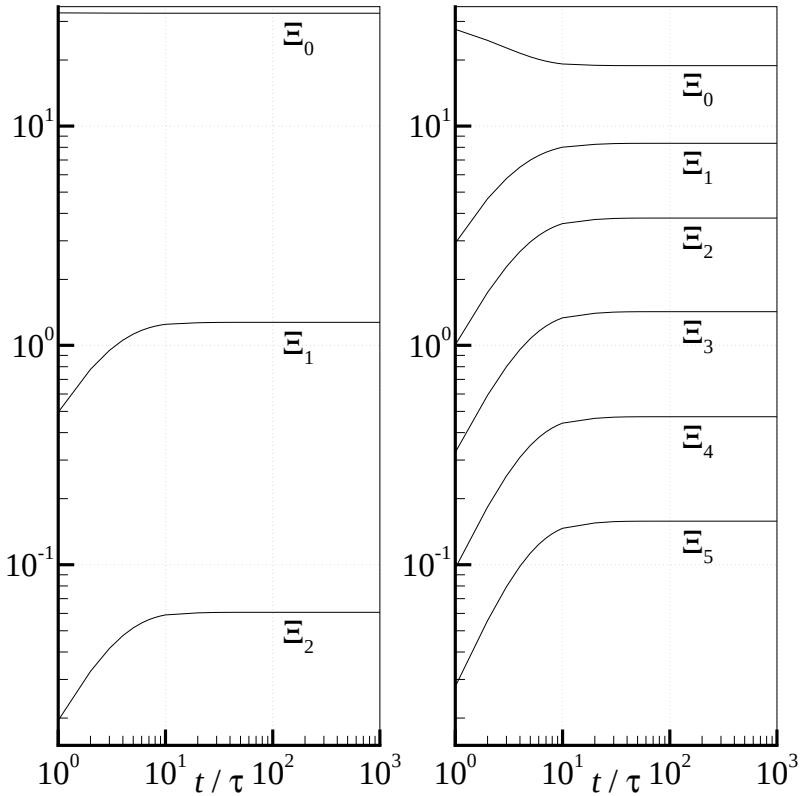

Figure: *Left:* Ξ_n where $V_{\mathrm{i}\perp} = 0.1\, v_{T\mathrm{i}}$ and $N = 2$. *Right:* Ξ_n where $V_{\mathrm{i}\perp} = v_{T\mathrm{i}}$ and $N = 5$.

θ-centered Implicit Time Advance

$$\Delta F_a - \theta \Delta t \sum_b \left\{ \Delta C_{ab} - \frac{2 f_a^{\mathrm{M}}}{m_a n_a v_{Ta}} \left[\mathbf{z}_a \cdot \Delta \mathbf{R}_{ab} + v_{Ta}^{-1} \left(\frac{2}{3} z_a^2 - 1 \right) \Delta Q_{ab} \right] \right\}$$
$$= \Delta t \sum_b \left\{ C_{ab} - \frac{2 f_a^{\mathrm{M}}}{m_a n_a v_{Ta}} \left[\mathbf{z}_a \cdot \mathbf{R}_{ab} + v_{Ta}^{-1} \left(\frac{2}{3} z_a^2 - 1 \right) Q_{ab} \right] \right\},$$

Field operator on right side of matrix equation:

$$-\frac{\Delta t}{2\pi} \frac{\Gamma_{ab}}{2} \int_\Omega d\mathbf{c}_a \mathrm{e}^{-in'\gamma} f_a^{\mathrm{M}} \left\{ -2 \frac{m_a}{m_b} \frac{v_{Tb}}{v_{Ta}} \overrightarrow{\alpha_j^{n'}} \cdot \nabla_{\mathbf{c}_b} \bar{h}_b \right.$$
$$-4 \left(\frac{v_{Tb}}{v_{Ta}} \right)^2 \left[\overrightarrow{\alpha_j^{n'}} \cdot \mathbf{z}_a + 2\alpha_j \left(1 - z_a^2 \right) \right] \bar{h}_b$$
$$\left. +4 \left(\frac{v_{Tb}}{v_{Ta}} \right)^3 \left[\overrightarrow{\alpha_j^{n'}} \cdot \mathbf{z}_a + 2\alpha_j \left(2 - z_a^2 \right) \right] \mathbf{z}_a \cdot \nabla_{\mathbf{c}_b} \bar{g}_b \right\}.$$

Spitzer Conductivity

The conductivity, σ, of the plasma is defined by the relationship

$$\mathbf{J} = \sigma \mathbf{E},$$

and can be calculated from the current and electric field. In an unmagnetized plasma,

$$\sigma = \alpha \frac{3\pi^{3/2}\varepsilon_0^2 m_\mathrm{e} v_{T\mathrm{e}}^3}{q_\mathrm{e}^2 \ln \Lambda_{\mathrm{ee}}},$$

where α has accepted values between 1.96 and 1.98.[1]

Spitzer Conductivity

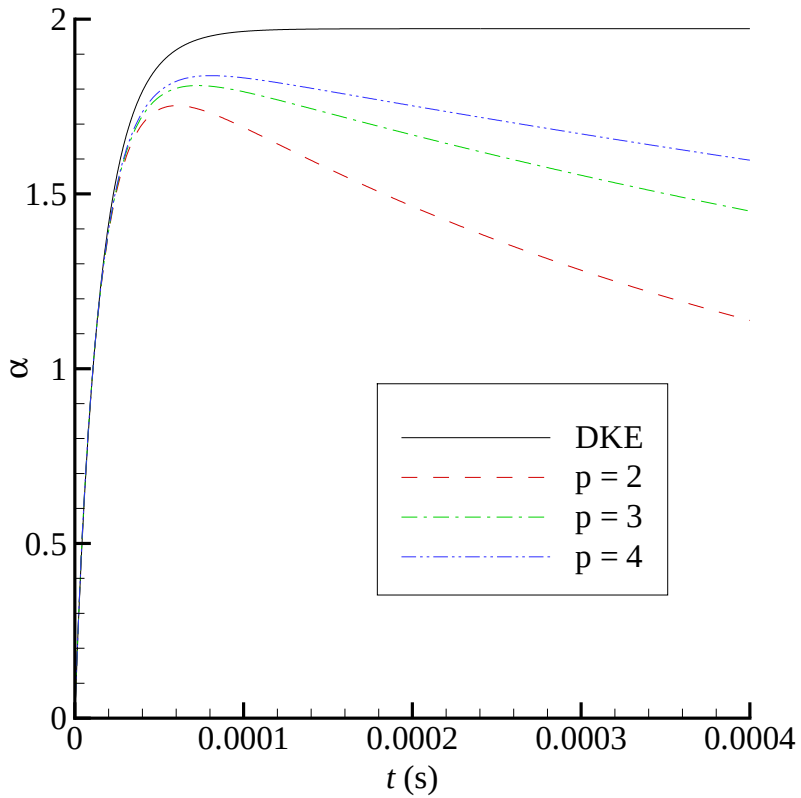

Figure: Evolution of conductivity coefficient, α, with $E = 10^{-2}\,\frac{\mathrm{V}}{\mathrm{m}}$, $n_\mathrm{e} = n_\mathrm{i} = 10^{19}\,\mathrm{m}^{-3}$, and initial $T_\mathrm{e} = T_\mathrm{i} = 200\,\mathrm{eV}$.

Grid Packing to Improve F_e Resolution

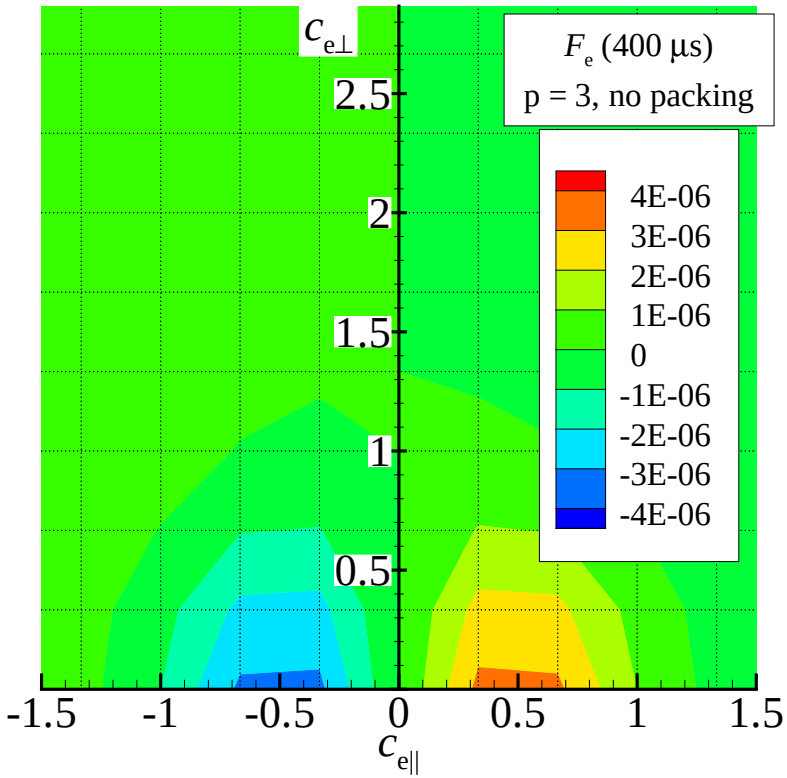

Figure: F_e after 400 μs with no grid packing, on a 4×12 grid.

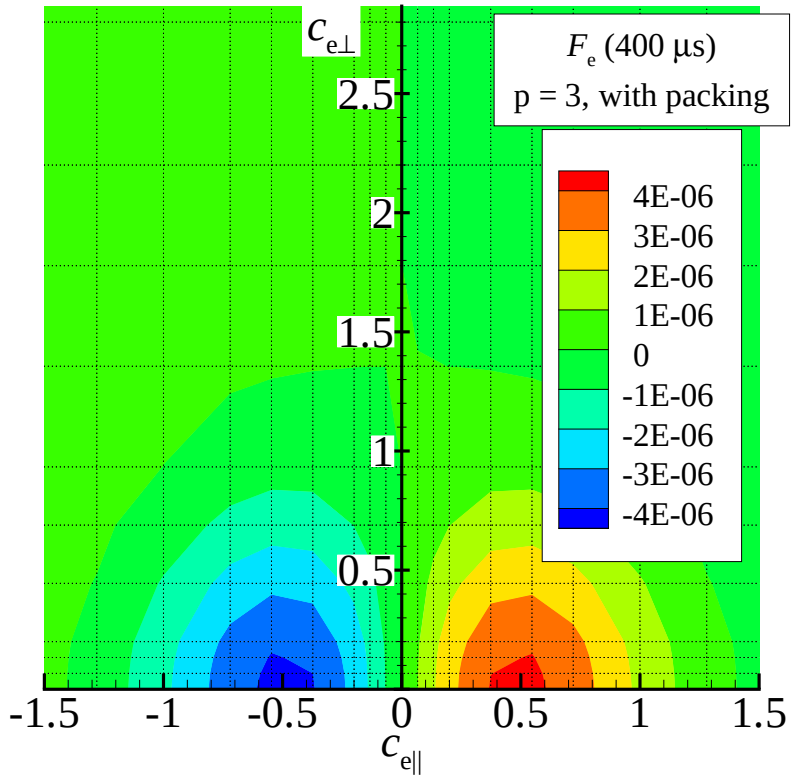

Figure: F_e after 400 μs with grid packing, on a 4×12 grid.

Spitzer Conductivity Improved with Grid Packing

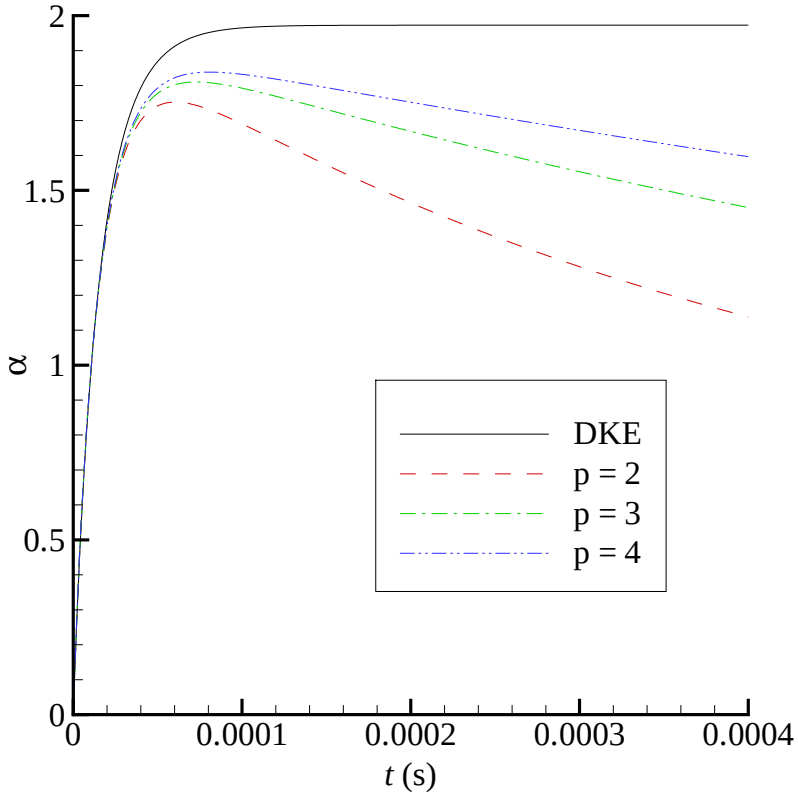

Figure: Evolution of α with no grid packing, on a 4×12 grid.

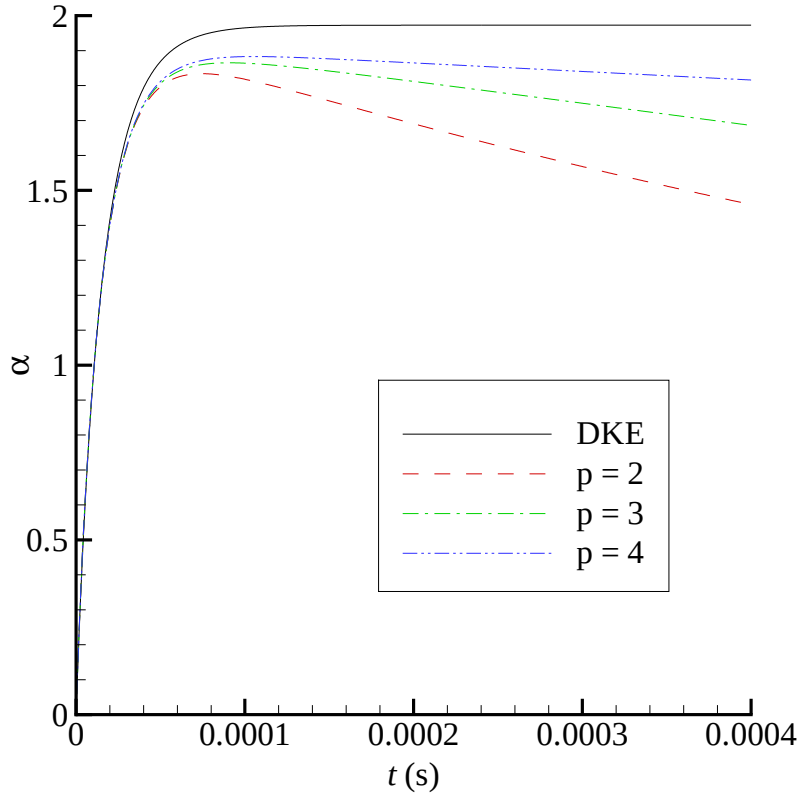

Figure: Evolution of α with grid packing, on a 4×12 grid.

Grid Packing on Semi-Circular Grid

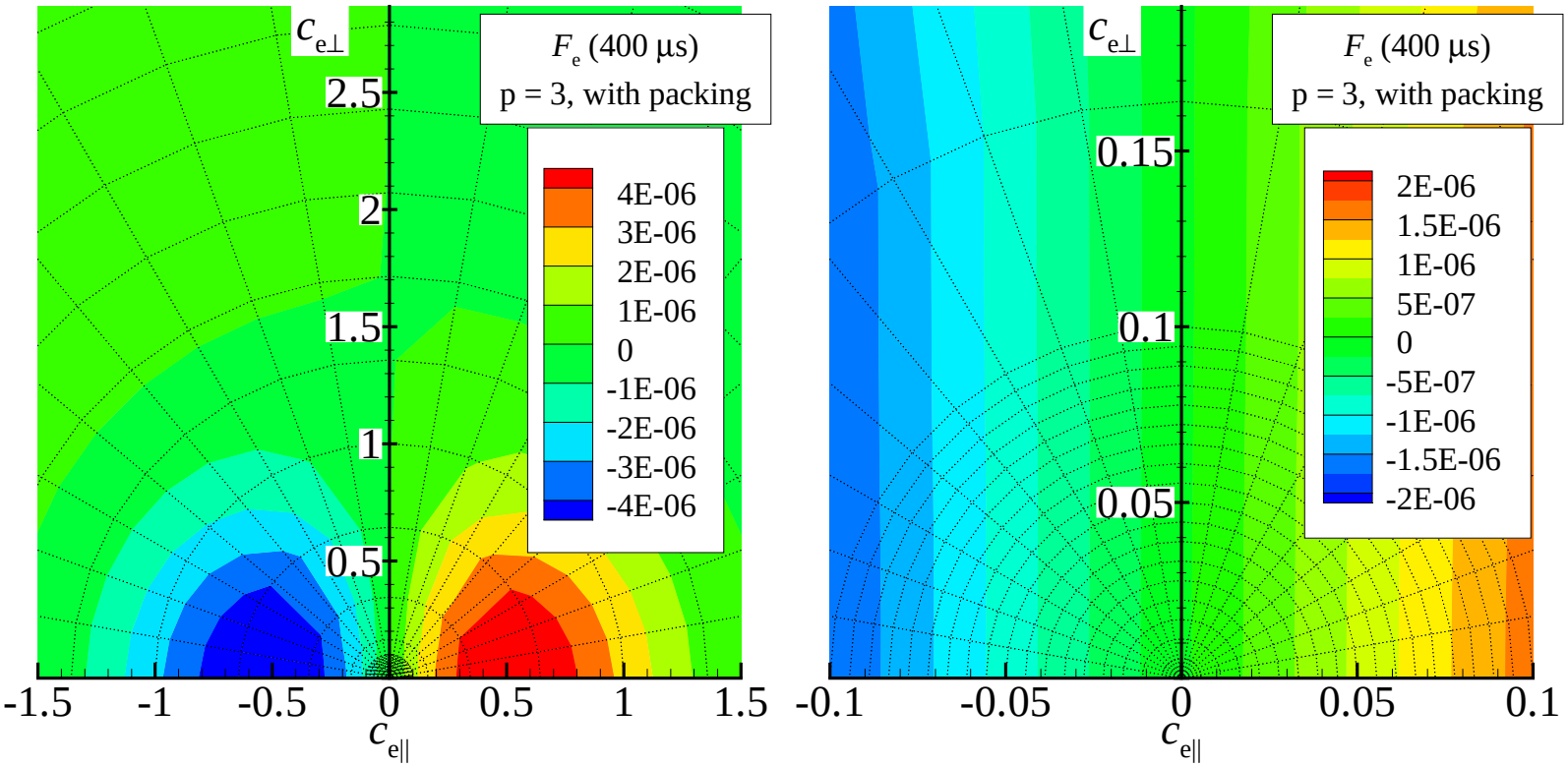

Figure: F_e after 400 μs with grid packing, on a 12×6 semi-circular grid.

Spitzer Conductivity Improved with Grid Packing

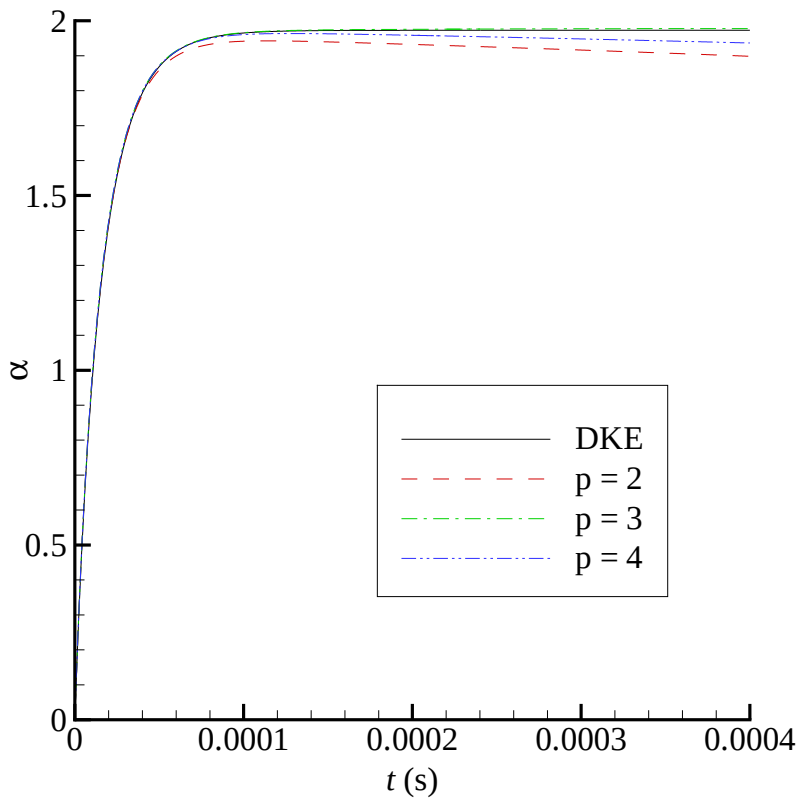

Figure: Evolution of α using semi-circular grid with grid packing close to the origin.

Spitzer Conductivity Improved with Grid Packing

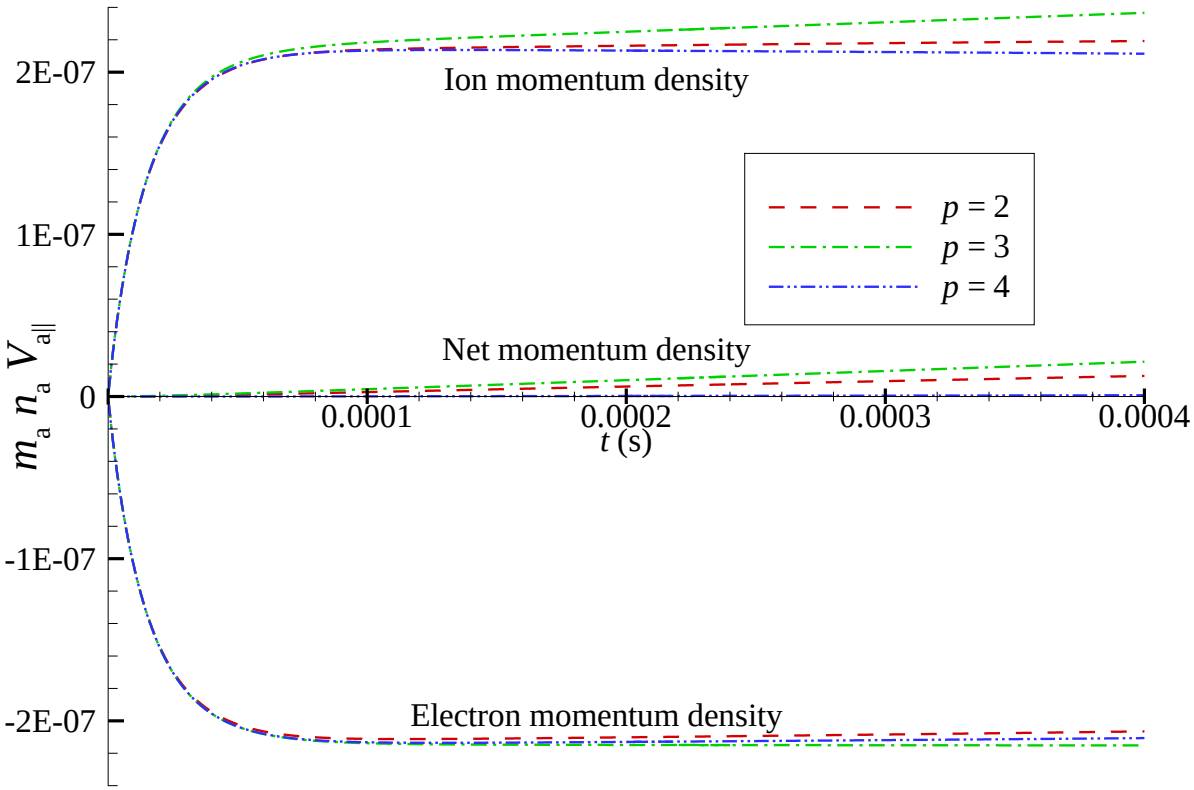

Figure: Momentum conservation for the conduction problem.

Spitzer Thermalization

Next, consider a plasma with electrons with an initial temperature,

$$T_{\mathrm{e}}\left(t=0\right)=205.4\,\mathrm{eV},$$

and ions with an initial temperature,

$$T_{\mathrm{i}}\left(t=0\right)=200\,\mathrm{eV}.$$

Spitzer Thermalization

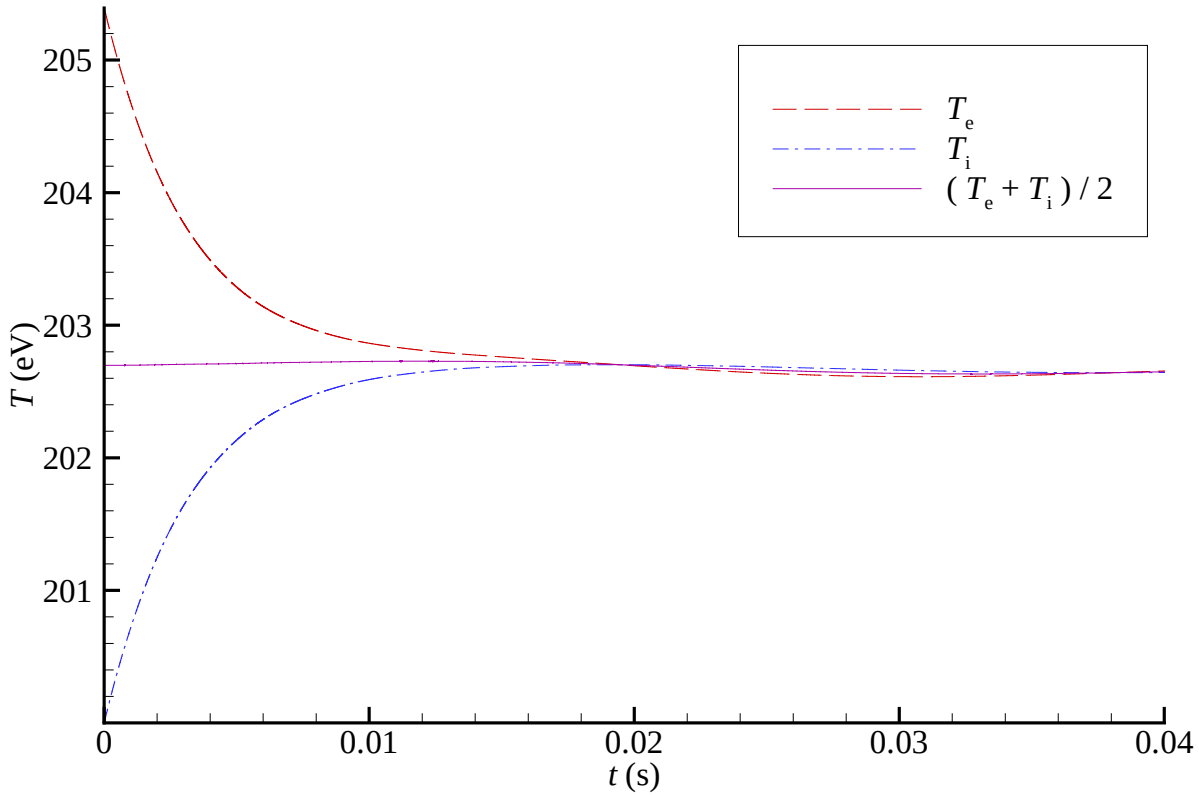

Figure: T_e and T_i, initially 205.4 eV and 200 eV respectively, and average temperature. $p = 2$ and a 6×8 grid was used over the domain $|\mathbf{c}_a| \leq 10$ (3×8 cells packed into a radius of $|\mathbf{c}_a| \leq 3$).

Summary & Future work

- We have a Fokker-Planck code implementing the *test particle operator* and the *field operator* both using θ-centered implicit time advance.
- Rectangular and semi-circular grids with grid packing can be used.
- The code can be executed in parallel over many processors.
- Numerical tests show good convergence properties and fidelity to conservation of properties of the collision operator.
- Future work under consideration:
  - More accurate/efficient calculation of TR potentials
  - Add spatial dimensions
  - Couple to NIMROD's fluid equations
  - Solve nonlinear kinetic equation